Helical Siberian Snakes and Spin Rotators for the HERA Proton Ring

D. P. Barber[a], V. Ptitsin[b], and Yu. M. Shatunov[c]

[a] Deutsches Elektronen-Synchrotron,DESY, 22603 Hamburg, Germany.
[b] Brookhaven National Laboratory, Upton, New York 11973, U.S.A.
[c] Budker Institute of Nuclear Physics, 630090 Novosibirsk, Russian Federation.

Abstract: Spin rotator and Siberian Snake configurations for the North and South interaction regions of the HERA proton ring are considered. Then designs for snakes and rotators based on sets of helical dipole magnets are proposed.

1 Introduction

According to numerical and analytical investigations [1, 2, 3] the HERA proton ring would require at least four Siberian Snakes in order to suppress the numerous depolarizing resonances occuring during acceleration and to maintain high polarization at the top energy. Furthermore, additional snakes are needed to effectively neutralise the sections containing interleaved vertical and horizontal bends at the ends of the arcs. These sections which we denote by "HVBS" then become transparent for vertical spins on the reference orbit so that the periodic polarization direction $\hat{\mathbf{n}}_0$ on the reference orbit is vertical in the arcs.

An important characteristic of a snake is the orientation of its axis of spin rotation. This is usually called the snake axis and we will describe it by the angle α between the axis and the longitudinal direction in the horizontal plane.

For an even number of snakes, distributed uniformly around the ring, and for a spin tune on the design orbit of one half, the directions of the snake axes must satisfy the following condition:

$$\sum_{i=\text{odd}} \alpha_i - \sum_{i=\text{even}} \alpha_i = \pm\frac{\pi}{2}$$

where the numbering of the snakes corresponds to the order in which a proton beam encounters the snakes while circulating in the ring.

Furthermore to provide longitudinal polarization at the North and South interaction points it would also be necessary to install two pairs of spin rotators in available free space around these IPs.

L1	L2	L3	L4	L5
10.3 m	11.4 m	13.3 m	16.5 m	34.8 m

Table 1: *Places available for snake (rotator) installation. Note that the lengths given are not the distances between bending magnets but the lengths of intervals free from quadrupoles.*

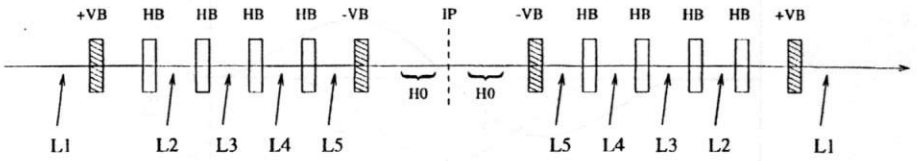

Figure 1: *The south (north) interaction region layout.*

2 Snake and rotator configurations

While the East and West interaction regions must only accommodate Siberian Snakes, in the North and South interaction regions one must also find free space for spin rotators. In this section we consider various possible snake and rotator arrangements in the North and South regions.

The layouts of the HVBS's at the ends of the arcs in the North (South) region mentioned earlier are sketched in Figure 1. Quadrupoles and other hardware between the magnets are not shown. If we assume that for a spin rotator or a snake one needs at least 10 metres of free space, there are only a few places available. These are indicated by arrows in Figure 1 and listed in Table 1.

The vertical bends ($\pm$VB) deflect the reference orbit by an angle of ± 5.74 mrad and the horizontal bends (HB) deflect it by 15.10 mrad. The spin rotation will be a factor of $\nu_0 = G\gamma$ larger and for the top HERA energies ($\nu_0 > 1500$) it is more than 8 radians in the vertical bends. Thus $\hat{\mathbf{n}}_0$ is not vertical in the arcs even without imperfections and has a very complicated dependence on energy [2]. In particular it can lead to difficulties in applying the Siberian Snake concept and it usually increases the number of strong depolarizing resonances. However, V. Anferov [4, 5] has proposed a way to compensate the effect of vertical bends by applying a "flattening snake", namely by including a snake with a radial axis in the interval L3. This converts each HVBS into a Siberian Snake with radial rotation axis. Another possible variant for flattening will be described below.

The additional horizontal deflection (H0) is due to the fact that the proton beam goes off centre through some interaction region quadrupoles of the electron ring. These provide an additional orbit deviation of about 0.28 mrad and correspondingly produce about 25° of spin rotation at the top energies. One immediate consequence of this additional spin rotation is that the rotators should set the spin in a direction in the horizontal plane which is not longitudinal and which is energy dependent. Two more problems are caused by the fact that this additional horizontal bending is symmetric with respect to the interaction point. Firstly, although vertical spin will be restored after traversing the pair of spin rotators, an additional spin rotation around the vertical direction can be acquired. As a consequence, the spin phase advance between Siberian Snakes is changed and the spin tune can deviate from the value of

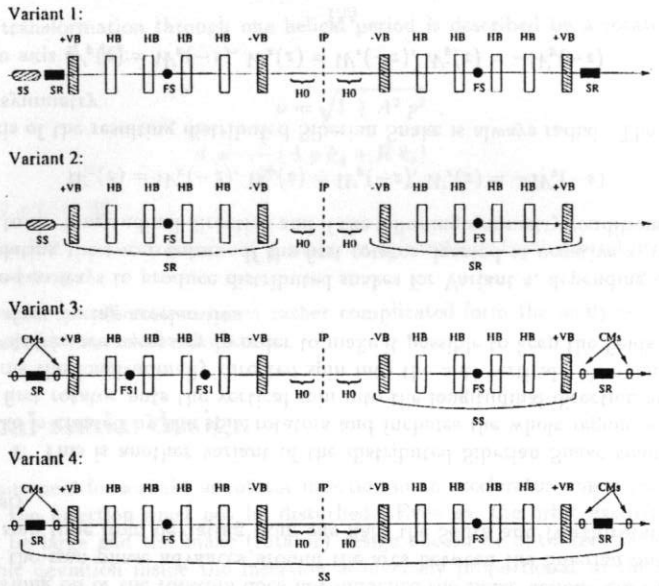

Figure 2: *The four variants of the possible snake and rotator configurations.*

one half. Secondly, while the rotator magnets are ramped to the required field level during the adiabatic turning-on procedure the symmetry relations between the two rotators can be broken. This would cause an additional shift of the spin tune away from one half and cause $\hat{n}_0$ to deviate from the vertical in the arcs. Thus special care must be taken when turning on the rotators.

One way to avoid these problems is to use additional horizontal correction bends, denoted by "CM", before and after each rotator. The correctors between the rotators and the interaction point, fully compensate the spin rotation from H0 and those between the rotators and the arcs compensate the resulting shift in the particle orbit. With these compensating magnets the rotator must only provide longitudinal spin at its exit, independently of the energy. We should also note that the use of the compensating dipoles also allows an operation regime in which the rotators are always turned on if the magnetic field of these compensating magnets is changed in proportion to the beam energy during acceleration.

We now discuss several possible snake and rotator configurations. Special attention will be paid to the symmetries of the rotator fields. The following definitions will be used. Let $W_x(z)$, $W_y(z)$ and $W_z(z)$ be components of the rate of spin precession in the rotators where x is the radial, y is the vertical and z is the longitudinal coordinate. The W_x and W_y are produced by horizontal and vertical magnetic field components of conventional or helical dipole magnets, and W_z can be associated with the helicity of a helical magnet [6]. Let us also place the symmetry point (interaction point (IP)) at $z = 0$, so that the first rotator is located at negative z and the second at positive z.

The various possibilities for snake and rotator configurations are sketched in Figure 2 :

Variant 1: In this configuration each separate device carries out its own specific task so that a full set of devices consisting of Siberian Snakes (SS), spin rotators (SR) and flattening snakes (FS) is needed. This configuration accounts for two of the total of required Siberian Snakes and they can have any required snake axis. On the other hand, each Siberian Snake must share a straight section with a spin rotator. Therefore the snake and the rotator must be short so that high magnetic fields are required. In the ideal situation, with compensating magnets installed, the second rotator must simply give a spin transformation which is the inverse of that of the first rotator:

$$W_x(z) = -W_x(-z),\ W_y(z) = -W_y(-z),\ W_z(z) = -W_z(-z) \tag{1}$$

In this case there are no problems with additional spin phase advance or with turning on the rotators.

However, with a snake and a rotator placed in one section, it is difficult to install compensating magnets in the same section. Without compensating magnets to restore the spin to the vertical after traversing the rotators the following symmetry is required:

$$W_x(z) = -W_x(-z),\ W_y(z) = W_y(-z),\ W_z(z) = W_z(-z) \tag{2}$$

One can show that in order to avoid additional spin rotation around the vertical direction, the spin transformation in each rotator must always have a rotation axis lying in the horizontal plane. Another possible solution is to always run the North and South region rotators simultaneously. Then additional spin phase advances acquired by a spin in these regions will cancel each other. But special care must be taken when turning on the rotators.

Variant 2: No rotators are included and the flattening snakes are used as snakes during acceleration. After that, the fields in the magnets of these snakes change to produce longitudinal spin at the interaction point. In fact, in this case, the HVBS is a spin rotator. Since the fields of the VB and HB dipoles depend on the beam energy, the fields of the flattening snake magnets, when such a section is operating as rotator, will depend on the working energy too. Also, there is no appropriate symmetry relating the magnet fields of two snakes for such rotators. Although this configuration seems rather complicated, it contains only three spin rotating devices instead of the five in the first variant described above.

Variant 3: The two previous configurations use Siberian Snakes, placed locally in a free straight interval of the ring. The required spin rotation is produced only by the magnets installed specially for this purpose. Also such a snake does not straddle quadrupoles. We call such a snake a "local snake".

The next two configurations to be presented use Siberian Snakes which contain both newly installed magnets and the bending dipoles of the HERA ring. Furthermore the Siberian Snake contains quadrupoles. Such a Siberian Snake will be called a "distributed snake". The flattening procedure gives us an obvious example of a distributed snake. Indeed, as was mentioned above, by using a flattening snake with a radial spin rotation axis a HVBS is turned into a Siberian Snake with radial axis. But because of the presence of two of these snakes around the interaction point, the spin rotation produced by the first snake is cancelled by the rotation in the second one.

Let us consider another way of effectively flattening the ring. If one positions two flattening snakes (FS1) in the left HVBS as shown in Figure 2 the spin transfer matrix for the whole

HVBS will be a unit matrix. Note that in this case the directions in the horizontal plane of the snake axes of the flattening snakes are arbitrary except that they must be identical. To prove this we treat the rotation produced by a flattening snake as a rotation of the coordinate frame rather than as a spin rotation. Then if both snakes have the same rotation axis the sequence of fields acting on the spin in the rotating frame will be:

$$(+\mathrm{VB},\ \mathrm{HB},\ -\mathrm{HB},\ -\mathrm{HB},\ \mathrm{HB},\ -\mathrm{VB}),$$

This obviously gives an identity transformation. After passing two flattening snakes the rotating coordinate frame coincides again with the laboratory frame.

Due to the presence of the flattening snake in the right HVBS, Variant 3 results in a distributed Siberian Snake with a radial spin rotation axis. Therefore this configuration can be applied if Siberian Snakes with radial axes are needed in the South or North sections of the HERA ring.

Note that in this configuration the Siberian Snake is located between the two rotators. The rotators are turned on after beam acceleration and an obvious requirement is that they must not disturb the spin rotation produced by the snake alone. This can be arranged in two possible ways.

If there are no compensating magnets the rotator fields must have odd symmetry:

$$W_x(z) = -W_x(-z),\ W_y(z) = -W_y(-z),\ W_z(z) = -W_z(-z) \tag{3}$$

and the rotation axis must lie in the horizontal plane. But, nevertheless, the spin transformation of the distributed snake can still be disturbed by turning on the rotators.

With compensating magnets before and after the rotators, the rotator fields have the symmetry relations:

$$W_x(-z) = -W_x(z),\ W_y(-z) = W_y(z),\ W_z(-z) = W_z(z). \tag{4}$$

Then the turning on of the rotators does not influence the snake action. On the other hand, they change the spin phase advances around the arcs between the Siberian Snakes. Thus to prevent the spin tune from deviating from one half, the South and North rotators would run simultaneously.

Variant 4: This is another variant of the distributed Siberian Snake concept. The distributed snake is created by the spin rotators and includes the whole region between the rotators. The first rotator puts the vertical spin into the longitudinal direction and the second one transforms the longitudinally directed spin into the anti-vertical. Compensating dipoles around the rotators are necessary in order to make it possible to keep the fields of the rotator magnets constant during acceleration.

There are two ways to produce distributed snakes for Variant 4, depending on the kind of symmetry relating the two rotators. If the first rotator, located at negative z, transforms the vertical spin to the longitudinal direction and if the following symmetry conditions are satisfied:

$$W_x(z) = W_x(-z),\ W_y(z) = W_y(-z),\ W_z(z) = -W_z(-z) \tag{5}$$

the snake axis of the resulting distributed Siberian Snake is always radial. The other variant involves the symmetry

$$W_x(z) = W_x(-z),\ W_z(z) = W_z(-z),\ W_y(z) = -W_y(-z) \tag{6}$$

In this case the snake axis α of the distributed snake depends on the rotator design (see section 5 for examples).

Of course, if distributed snakes are used, it is important to know how the presence of quadrupoles, and hence, sources of spin perturbation inside the snake affect the ability of the snake to damp spin perturbations.

Each of the four configurations presented has its own positive and negative aspects and the most appropriate choice must be the subject of further studies.

Now that several configurations of snakes and rotators have been suggested, the next step is to find the most appropriate designs for each individual snake and rotator. In the following sections designs based on the use of helical dipole magnets are discussed. Variants based on conventional dipole magnets can be found in [4, 7].

3 Some facts about spin and orbital motion in helical magnets

Let us briefly list some facts regarding spin and orbital motion in a helical dipole magnet.

Assuming that the magnetic field is vertical at the entrance of a helical magnet with helical period λ (metres), we will approximate the field with the on-axis field namely:

$$B_x = -B_0 \sin kz\ ,\quad B_y = B_0 \cos kz\ ,\quad B_z = 0 \tag{7}$$

where $|k| = 2\pi/\lambda$. The sign of k determines the helicity of the magnet ($R = k/|k|$). Note that this simplified representation does not satify Maxwell's equations off axis. Nevertheless this approximation suffices to demonstrate the main points that we wish to make. A more accurate representation can be found in [8].

By solving the equation of particle motion in the paraxial approximation the transformation of the particle orbit for one period is found to be [6]:

$$\begin{aligned} x &= x_0 + x_0'\lambda\ ,\quad x' = x_0', \\ y &= y_0 + y_0'\lambda - \frac{p}{\gamma} R\lambda\ ,\quad y' = y_0' \end{aligned} \tag{8}$$

where p is the field parameter defined as

$$p = \frac{q_0 B_0}{c|k|} \tag{9}$$

with $q_0 = e/mc$ and where the subscript "0" indicates entrance coordinates. In fact the quantity p is the (dimensionless) field integral over one period of a helical magnet. B_0 and, therefore p can take positive and negative values. For protons, $p = 1$ corresponds to a field integral of 19.665 Tm.

For particles entering the magnet parallel to its axis ($x_0' = 0, y_0' = 0$), after one period the orbit is simply shifted along a direction determined by the magnetic field vector at the entrance to the magnet. The orbit shift can be negative or positive depending on the sign of the product pR.

The spin transformation through one helical period is described by a rotation angle $2\pi\nu$ and a rotation axis $\vec{n}$ [1] [6]:

$$\nu = \sqrt{1 + \Lambda^2 p^2} \tag{10}$$

$$\vec{n} = -\frac{1}{\nu}(A\, p\, \hat{\mathbf{e}}_y + R\, \hat{\mathbf{e}}_z)$$

where $\Lambda = (G + 1/\gamma)$ [8].

Using these facts one can construct a snake or spin rotator from several helical modules, each one period long.

Since the spin transformation has a rather complicated form the analysis of the possible schemes is made by numerical calculation.

4 Helical snake design

The first requirement for a snake or rotator insertion in an accelerator ring is that the particle orbit outside the insertion must not be disturbed. Even so, the orbit excursion inside the insertion can be large and the snake (rotator) design should be optimized to minimize this. Since the orbit deviation inside the insertion is inversely proportional to the proton beam energy, the orbit deviation should be analyzed at the injection energy. Thus in the following, the orbit deviation will refer to the HERA injection energy of 40 GeV.

The matter of the best choice of snake axis configuration for damping spin perturbations is still open [10]. Therefore we will consider snake designs with various snake axis orientations. In particular we consider two ways to apply symmetry conditions to design a helical snake.

4.1 Continuously variable snake axis

We begin with a snake with a continuously variable horizontal snake axis that restores the orbit after the snake. This snake is based on a special field symmetry [11] and can, for example, be realised using four helical magnet modules [12]. In terms of the parameters of helical magnets the symmetry requires that the magnetic field at the entrance and exit of each helical magnet must be vertical and that:

$$R(z) = R(-z)\,, \quad p(z) = -p(-z) \tag{11}$$

where $z = 0$ corresponds to the midpoint of the snake.

The best variant of the design for a continuous axis helical snake is presented in Figure 3. The 45° version of this snake has been accepted for use on the RHIC collider at BNL [13]. The values of the field parameters p_1 and p_2 (equation 9) required to obtain the snakes axis angle α can be read from Figure 4 (left) [2]. Table 2 lists the field values, the maximum orbit excursion inside the snake (at 40 GeV) and the field integral for 0°, 45° and 90° snakes axes,

[1] These symbols ν and $\vec{n}$ are not to be confused with spin tune ν and the invariant spin field $\hat{\mathbf{n}}$ commonly used for describing spin dynamics in accelerators [9].

[2] Here, the snake axis angle α is the angle between the longitudinal direction ($\hat{\mathbf{e}}_z$) and the negative x direction ($-\hat{\mathbf{e}}_x$).

α	B_1 (T)	B_2 (T)	integral(Tm)	y_{max}(cm)
0°	2.191	-2.907	24.47	1.5
−45°	3.564	-1.618	24.88	2.4
45°	1.259	-4.043	25.45	1.9
90°	4.761	-1.332	29.25	3.3

Table 2: *Parameters for a continuous axis helical snake and for some selected snake axis directions.*

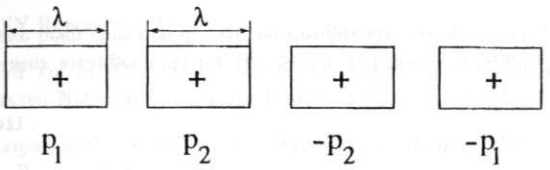

Figure 3: *The design for the continuous axis helical snake. The sign (+) denotes the magnet field helicity.*

assuming a helical period length of $\lambda = 2.4$ m. Reduction of λ results in a proportional decrease of the orbit excursion and in a proportional increase of the magnetic field required. Note that only positive p_1 (and hence B_1) values have been shown in Figure 4 (left) and Table 2. The solutions with negative p_1 can be easily obtained by a 180° rotation of the whole snake around the longitudinal axis. Then $p_1 \to -p_1$, $p_2 \to -p_2$ and $\alpha \to -\alpha$.

From Table 2 it can be seen that the largest field integral as well as the largest orbit deviation correspond to the radial (90°) snake. This brings us to our second case, namely an alternative design for a radial snake.

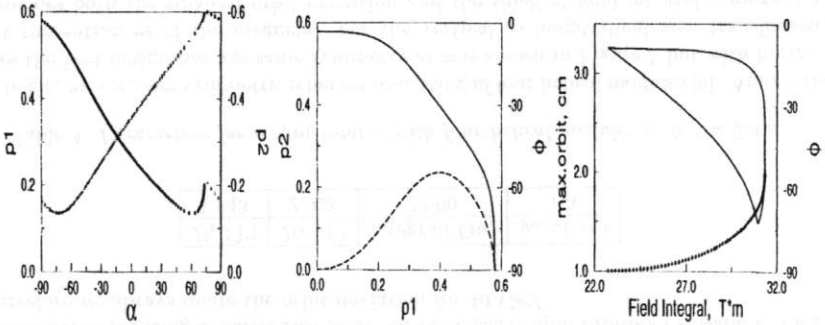

Figure 4: Left: *The dependence of the field parameters p_1 (o) and p_2 (+) on the snake axis angle α.* Middle: *The relationship between p_1 and p_2 (solid line), and the corresponding field orientation angle ϕ (dashed line) to get a radial snake.* Right: *The relationship between the field integral value and the maximum orbit deviation (solid line), and the corresponding field orientation angle ϕ (+) for the radial snake.*

ϕ	B_1 (T	B_2 (T)	integral(Tm)	y_{max}(cm)
$-66.9°$	2.148	4.296	30.94	1.5
$-55.5°$	3.264	3.264	31.33	2.2
$-90°$	0.	4.738	22.74	3.3

Table 3: *Parameters for some variants of the radial snake.* $\lambda = 2.4m$.

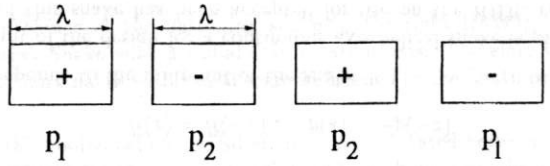

Figure 5: *The design of the radial snake. The signs inside the boxes denote the magnet helicity.*

4.2 Radial snake

Let us consider again a snake consisting of four helical magnets but this time with the symmetry:

$$R(z) = -R(-z)\,, \quad p(z) = p(-z) \tag{12}$$

The magnetic field at the entrance and exit of each helical magnet is again vertical. Then one automatically gets a snake axis lying in the plane orthogonal to the longitudinal axis of the magnets, as well as orbit restoration after the snake. Obviously any such scheme can be transformed to a radial snake by simple rotation of the whole scheme around the longitudinal axis or, in other words, by proper choice of the magnetic field direction at the entrance of the helical magnets. We will characterize this direction by the angle ϕ between the vertical axis ($\hat{\mathbf{e}}_y$) and the negative x axis ($-\hat{\mathbf{e}}_x$).

Note that there are two schemes of this kind: when the helicities of the first and second helical magnets are the same and when they are different. A numerical analysis has shown that the latter is the preferable variant from the point of view of the orbit deviation and the field integral. This design is sketched in the Figure 5. Figure 4 (middle) shows the dependence of the field parameters p_1 and p_2 on the corresponding field orientation angle ϕ. Table 3 lists the parameters for three variants: with minimal particle orbit deviation, with minimal value of the magnetic field required and with a minimal value of the field integral. Note that the last scheme consists in fact of only two helical magnets (hence it is a factor of two shorter) and uses magnets with radial fields at their entrances. In Figure 4 (right) the relation between the maximum orbit excursion and the total field integral is shown. This can be used to select a compromise variant.

As mentioned above (Variant 2 in Fig. 2) the flattening snake can be used after beam acceleration as a component of a spin rotator. In this case the required fields of the helical magnets of the snake depend on the energy at which the rotator is operating. Analysis of the helical radial snake designs has shown their ability to operate as a part of a rotator, but at some beam energies excessively large magnetic fields (B_1, B_2) are needed to produce the correct spin rotation.

5 A helical spin rotator

In this section we consider the design of a rotator which rotates proton spin from the vertical to the longitudinal direction.

If the rotators are only to be used at the top HERA energy the orbit excursion is not such an important issue. Thus the main issues for the analysis of possible spin rotator schemes are the total field integral and the maximum required field value. Nevertheless we will keep in mind the possibility of realising a distributed snake on the basis of spin rotators (Variant 4 in Fig. 2) and therefore we always quote the orbit deviation for 40 GeV.

B_1 (T)	B_2 (T)	integral(Tm)	y_{max}(cm)
1.843	2.928	22.90	1.3

Table 4: *Parameters for a spin rotator with four helical modules with* $\lambda = 2.4m$.

To begin, we consider symmetric schemes consisting of four helical modules [6]. Among these schemes the best design has the same symmetry as was shown in Figure 5 but with horizontal field at the entrances of the magnets. For the vertical to longitudinal spin transformation this provides both the smallest orbit excursion and the smallest field integral compared with other schemes of this kind. The parameters of this rotator are shown in Table 4. The spin transformation in the rotator is actually a 90° rotation around the radial axis. Thus distributed snakes realised on the basis of this rotator, which are created in both ways described in section 2 (Variant 4), have radial axes too.

We also considered rotators comprising three helical dipoles with the aim of reducing the field integral. Three variants with similar values for the field integral and the orbit deviation have been found. Their designs are shown in Figure 6 and their parameters are listed in Table 5.

The value of α in the table is the angle of the snake axis for a distributed snake created in the second way described in section 2 (Variant 4) for a particular design of the rotator. Thus two snakes have nearly longitudinal snake axes and one snake has almost a $-45°$ snake axis.

Finally, we note that to transform vertical spin to the negative longitudinal one only has to reverse the fields of the helical magnets.

6 Conclusion

Several snake and rotator arrangements for the South and North interaction regions of the HERA proton ring have been considered. All the designs are based on helical magnets. The

Variant	B_1 (T)	B_2 (T)	B_3 (T)	integral (Tm)	y_{max}(cm)	α
1	-1.708	4.137	2.429	19.86	1.7	-2.5
2	2.598	3.843	1.245	18.45	1.8	-44.8
3	2.512	4.062	-1.550	19.50	1.7	-5.7

Table 5: *Parameters for three helical modules spin rotators.* $\lambda = 2.4m$.

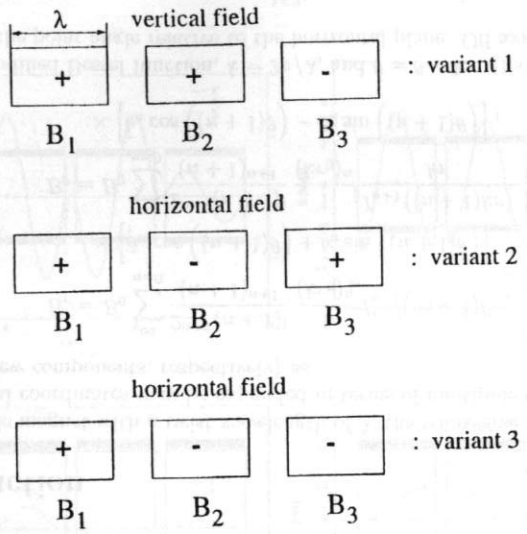

Figure 6: *Designs of spin rotators consisting of three helical magnets.*

choice of the final configuration is a matter for further analysis. Such schemes usually provide less orbit deviation inside a snake (rotator) than schemes based on conventional dipole magnets. Helical snakes and rotators have been accepted for use in the RHIC accelerator at BNL [13] and they are currently under construction.

Naturally, the actual fields of helical dipoles are more complicated than those used here for investigation of spin and orbit motion in paraxial approximation. Maxwellian fields should be used and fringe fields should be taken into account. More precise values for the required magnetic fields must be obtained by direct integration of particle and spin motion in real helical fields [14]. Investigations made for RHIC led to the conclusion that magnets with 345° helical field twist should be used rather than magnets with full (360°) twist.

References

[1] M. Vogt, thesis in preparation.

[2] V. Balandin, N. Golubeva, D.P. Barber, DESY report M-96-04 (1996).

[3] V. Balandin, D.P. Barber, N. Golubeva, DESY report M-98-03 (1998).

[4] SPIN at HERA Collaboration (L.V. Alekseeva et al.), University of Michigan report UM-HE-96-20 (1996).

[5] V.A. Anferov and R.A. Phelps, Nuclear Instruments and Methods, **A398** (1997) 423.

[6] V. I. Ptitsin and Yu. M. Shatunov, Nuclear Instruments and Methods, **A398** (1997) 126.

[7] V.A. Anferov, article in these Proceedings.

[8] E.A. Perevedentsev, V.I. Ptitsin and Yu.M. Shatunov, Proc. of 1992 Part. Accel. Conf., Hamburg, vol.1, (1992) 170.

[9] M. Vogt, article in these Proceedings.

[10] G. H. Hoffstätter, article in these Proceedings.

[11] K. Steffen, DESY Report 83-124 (1983).

[12] V. I. Ptitsin and Yu. M. Shatunov, Proc. of 3rd Workshop on Siberian Snake and Spin Rotators, Brookhaven National Laboratory Report BNL-52453 (1994).

[13] *Conceptual Design for the Acceleration of Polarized Protons in RHIC* , Brookhaven National Laboratory Report (1995).

[14] A. Luccio, Proc. of 3rd Workshop on Siberian Snakes and Spin Rotators, Brookhaven National Laboratory Report BNL-52453 (1994).

Development of the BINP type atomic injector for the OPPIS

V. I. Davydenko

Budker Institute of Nuclear Physics, 630090, Novosibirsk, Russia

Abstract: The BINP type atomic injectors with high beam brightness are adequate for use in optically pumped sources of polarized ions for accelerators. A focused atomic beam is to be injected into a solenoid of a polarized ion source to produce polarized ions by combination of charge-exchange and spin exchange mechanisms. The magnetically focused beam of hydrogen atoms with energy 5–7 keV has been successfully tested in model experiments for the pulsed optically pumped source at TRIUMF. By now the 6 mA level of polarized ion current has been achieved at the polarized source. In the report a problem of beam space charge compensation in a magnetic lens is discussed. Realization of geometrical focusing of the atomic beam using an ion optics system with spherical bent electrodes is considered. A version of an arc plasma generator with intense water cooling of discharge chamber parts operated at 2 s pulse duration is presented.

BINP type atomic injectors have been developed for plasma diagnostics in magnetic fusion experiments. Series of injectors of focused neutralized ion and atomic beams with beam energy ranging from 5 to 40 keV, equivalent beam current of 1–20 A, angular divergence of the beam $\sim 10^{-2}$ rad, equivalent current density in the focus of the beam more than 1 A/cm^2, pulse duration of 0.1–100 ms have been produced in Budker Institute of Nuclear Physics. The BINP type atomic injectors are also effective for application in optically pumped sources of polarized ions [1, 2]. At present the 6 mA current of polarized ions has been achieved at the polarized source at TRIUMF. Model approaches, results on magnetic and geometrical focusing of atomic beams and suggestions to achievement of 20 mA current of polarized ion are presented in the report.

Specific approach to formation of high brightness ion beams based on the use of a plasma emitter with low transverse ion temperature and precise beam formation is applied in these injectors. The low transverse ion temperature of the plasma emitter is achieved by the use of the plasma emitter formed by a collisionlessly expanding plasma jet. Fig. 1 shows the experimental arrangement of the plasma emitter.

The plasma, which comes out from a small anode opening of diameter $2R_0 \sim 0.5$ cm of a cold cathode arc source with a density $n_0 \sim 10^{14}$ cm^{-3} and ion temperature of ~ 3–5 eV, expands freely into vacuum. Consideration of classical collisions [3] in the stream shows that beyond a distance $r_0 \sim 1$ cm the flow of the ion component of the plasma becomes collisionless. In the first approximation we can assume that at distances greater than r_0 the ions move along

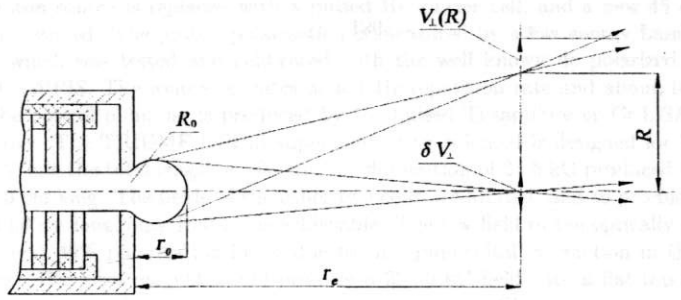

Figure 1: *Scheme of the plasma emitter.*

straight-line trajectories. In this case, in the plane of the plasma electrode of the ion optics system located at a distance r from the anode, an ion flux is produced which has a regular radial velocity $v_\perp(R) \approx v_i R/r_e$ (R is the distance from the beam axis) with a thermal spread $\delta v_\perp \approx v_i r_0/r_e$. Thus, the transverse temperature of the ions of the emitting plasma defined as $T_\perp \approx M\delta v_\perp^2/2$ (M is the ion mass) is reduced by a factor $(r_e/r_0)^2 \gg 1$ in comparison with the ion temperature close to the anode hole. The existing regular radial velocity of the ion flux does not contribute to the magnitude of the phase space of the produced ion beam and is equivalent to the action of a diverging lens with a focal length $f = -r_e v_b/v_i$, where v_b is the velocity of the beam ions.

An experimental check of the approach described was carried out on the basis of the diagnostic hydrogen-atoms injector. The beam was formed by a multi-slit four-electrode system [4] placed at a distance $r_e \sim 5$ cm from the anode aperture of the arc source. The electrodes of the ion optics system are tense molybdenum wires 0.2 mm in diameter spaced at 1 mm, the gap between the plasma electrode and the extracting one is 5 mm. Measurements of the local angular divergence of the formed beam of protons with energy 10 keV performed in the direction along the slits of the shaping system showed that the beam has a regular radial divergence $\partial\alpha/\partial R \approx 6 \cdot 10^{-3}$ rad/cm and an angular spread $\delta\alpha \approx 4.5 \cdot 10^{-2}$ rad corresponding to a proton transverse temperature $T_\perp \approx 0.2$ eV. The numerical values of these quantities are rather well within the estimates given above.

At study of magnetic focusing the proton beam of diameter $2R_e = 4$ cm was focused by a magnetic lens and was charge-exchanged into atoms in a target with pulsed hydrogen puffing. The distance between the ion optics system and the magnetic lens in the experiments was $L_1 = 20$ cm and the distance between the lens and the plane of measurement was $L_2 = 80$ cm. The minimum half-width R_2 of the beam in the direction along the slits of the ion optics system for optimal focusing should be determined by the following relation: $R_2 = L_2/(1 + L_1\partial\alpha/\partial R)$. After substitution of the values given above for $\partial\alpha/\partial R$ and $\delta\alpha$ we obtain $R_2 = 3.2$ mm. The measured half-width (at the $1/e$ level) of the focused atomic beam was 3.4 mm, in good agreement with the calculated value of R_2. The half-width of the focused beam in the direction across the slits was 13 mm and is also in agreement with the measured local angular divergence. At beam energy of 15 keV corresponding to the maximum amplitude of the extracting-voltage pulse from the injector used, a proton beam with a current of 2.5 A was obtained from the source. The normalized brightness of the proton beam, calculated according to the formula

[5] $B = \frac{2I_b c^2}{\pi^2 \delta\alpha_x \delta\alpha_y R_e^2 v_b^2}$, where I_b is the beam current, $\delta\alpha_x$ and $\delta\alpha_y$ are the angular spreads in the direction along and across the slits respectively, is $1.1 \cdot 10^8$ A/cm^2 rad^2. The corresponding atomic beam had an equivalent current of 2 A and a maximum current density of 1.7 A/cm^2 at a distance 1 m from the injector.

It was experimentally found that at beam energy below 4 keV the magnetic focusing of the ion beam is slightly reduced due to insufficient beam space charge compensation by secondary electrons in the magnetic lens. To compensate the beam space charge in the lens magnetic field at low beam energy, a high transparency copper grid emitting secondary electrons with biasing at $U \approx +50$ V is installed inside the lens. In the OPPIS investigations at TRIUMF [2] it was revealed that injection of electronegative CO_2 gas into the magnetic lens further improves compensation and increases the current into Na cell approximately by 20%.

Another approach to produce focused atomic beams is geometrical focusing. This approach allows one to avoid the problem of beam space charge compensation at low energies. The focused beam is formed by an ion optics system with spherically bent electrodes (Fig. 2).

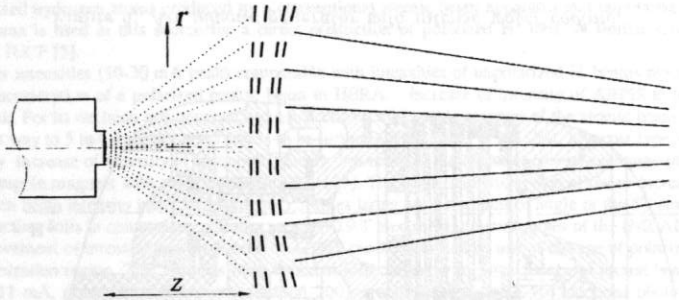

Figure 2: *Formation of an ion beam with geometrical focusing.*

The developed ion optics systems with geometrical beam focusing have gaps extending with radius which provides optimal beam formation from enlarged surface. The bell-like radial distribution of the proton current density in a plasma jet is approximated by the expression $j(r) = \frac{I}{\pi^2 z^2 (1+r^2/z^2)}$ [6], where I is the total proton current in the jet, z is the distance to the generator along the axis, and for optimal formation of the proton beam in agreement with the law of Child–Langmuir the following increase of gaps of the ion optics system with radius is required: $d(r) = d_0(1+r^2/z^2)$, where d_0 is the value of the gap at the axis. The multi-aperture ion optics system consists of four spherically bent electrodes. The curvature radii of the first three electrodes — plasma, extracting and accelerating are different, which provides the increase of the gaps with radius reasoned above. The curvature radius of the fourth grounded electrode coincides with the curvature radius of the accelerating one. For determination of the focus distance at given geometry of the ion optics system it is necessary to take into account a series of factors: difference in radii of the electrodes, position of the plasma boundary in an elementary cell, initial velocity of ions in the plasma emitter, compression of an elementary beam at an exit. These factors were correctly analyzed in three-dimensional numerical calculations of elementary beam formation in the ion optics system by Niemel and Whealton from ORNL [7] and results of these calculations are in good agreement with the obtained experimental data.

Four variants of the ion optics system with geometrical focusing have been developed. The parameters of these systems are presented in the Table.

E, keV	I, A	D, cm	$\delta\alpha$, 10^{-2} rad	τ, ms
8	17	14	1.7	100
30	2.5	7	1.2	20
40	1.5	7	1.2	20
30	4.5	8	1.1	3

The holes in the grids of the first three variants of the ion optics system are produced by drilling and in the fourth variant the holes in the grids are made by photoetching technology. The technology of photoetching allows one to produce thin grids with large number of holes. The grids are shaped under stress at high temperature.

Variant of an ion optics system with geometrical focusing for the atomic source of the OPPIS at TRIUMF is suggested. Fig. 3 shows the view of the grid which should be produced by photoetching way.

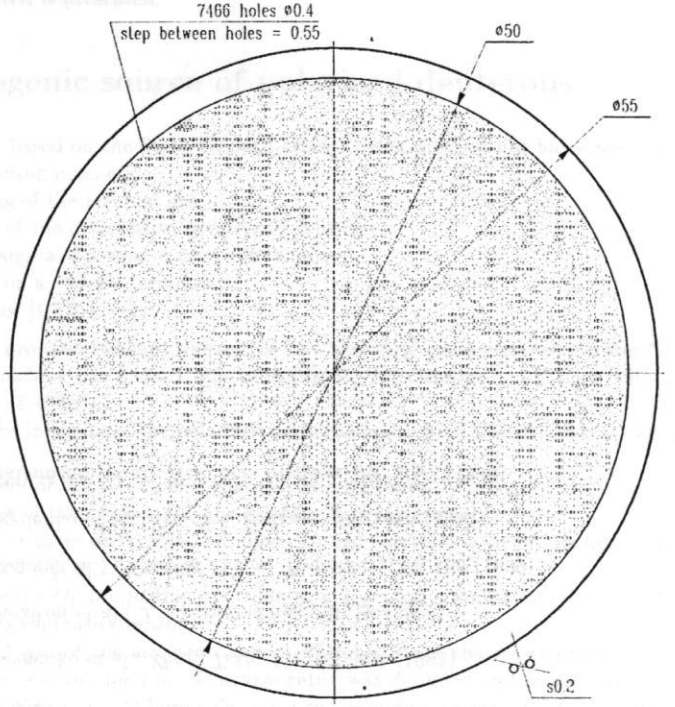

Figure 3: *Ion optics grid for the OPPIS.*

The ion optics system is intended to form a proton beam with energy of 5 keV, beam current of 5 A, angular divergence of the beam $1.5 \cdot 10^{-2}$ rad. Estimates show that the use of this ion optics system in the TRIUMF OPPIS allows achievement of 35 mA current of polarized ions. Of course, the experimental check of the suggested variant of the ion optics system at the OPPIS is necessary.

Though the existing version of the atomic injector has short pulse duration of 200 μs, two recently obtained important experimental achievements permit increasing of the pulse duration of geometrically focused beams up to several seconds. A version of an arc plasma generator with intense water cooling of discharge chamber parts (Fig. 4) has operated at 2 s pulse duration [8].

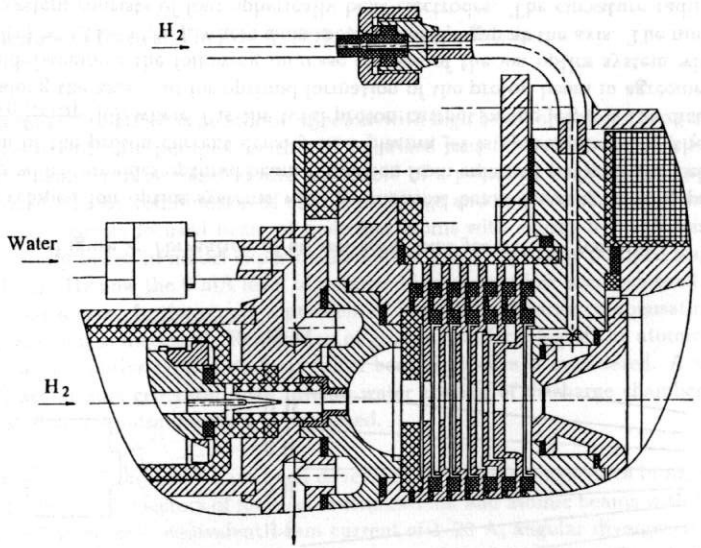

Figure 4: *Arc plasma generator with intense water cooling.*

The ion optics system with "thick" grid electrodes and peripheral cooling [9, 10] providing geometrical focusing of the formed ion beam has been developed and successfully tested at 4 s pulses.

In conclusion it should be said that the use of the ion optics system with geometrical focusing in the BINP atomic source and the change of the superconducting solenoid allows achievement of the 20 mA level of polarized ion current in the OPPIS at TRIUMF. After that BINP can develop, produce and test the optically pumped source of polarized ions for DESY.

References

[1] A. N. Zelenski et al., *Rev. Sci. Instrum.* **67**, 1359 (1996)

[2] C. D. P. Levy and A. N. Zelenski, *Rev. Sci. Instrum.* **69**, 732 (1998)

[3] Yu. I. Belchenko et al., *Rev. Sci. Instrum.* **61**, 378 (1990)

[4] V. I. Davydenko, *Nucl. Instrum. Methods* A **427**, 230 (1999)

[5] M. D. Gabovich. Physics and technology of plasma sources of ions (Atomizdat, Moscow, 1972) p. 304

[6] V. I. Davydenko et al., *Zhur. Tekh. Fiz.* **53**, 258 (1983)

[7] J. H. Whealton et al., *J. Comput. Phys.* **63**, 20 (1986)

[8] A. A. Ivanov et al., *Trans. of Fusion Technology* **35**, 180 (1999)

[9] V. I. Davydenko et al., *Rev. Sci. Instrum.* **68**, 1418 (1997)

[10] A. D. Beklemishev et al., *Rev. Sci. Instrum.* **69**, 2007 (1998)